Separation Science and Technology
Publication details, including instructions for authors and subscription information:
http://www.informaworld.com/smpp/title~content=t713708471

Adsorption Characteristics of Chitosan-*g*-Poly(acrylic acid)/Attapulgite Hydrogel Composite for Hg(II) Ions from Aqueous Solution

Xiaohuan Wang[ab]; Aiqin Wang[a]
[a] Center of Eco-Material and Green Chemistry, Lanzhou Institute of Chemical Physics, Chinese Academy of Sciences, Lanzhou, P. R. China [b] Graduate University of the Chinese Academy of Sciences, Beijing, P. R. China

Online publication date: 15 September 2010

To cite this Article Wang, Xiaohuan and Wang, Aiqin(2010) 'Adsorption Characteristics of Chitosan-*g*-Poly(acrylic acid)/Attapulgite Hydrogel Composite for Hg(II) Ions from Aqueous Solution', Separation Science and Technology, 45: 14, 2086 — 2094
To link to this Article: DOI: 10.1080/01496395.2010.504436
URL: http://dx.doi.org/10.1080/01496395.2010.504436

Separation Science and Technology, 45: 2086–2094, 2010

ISSN: 0149-6395 print/1520-5754 online
DOI: 10.1080/01496395.2010.504436

Taylor & Francis
Taylor & Francis Group

Adsorption Characteristics of Chitosan-*g*-Poly(acrylic acid)/ Attapulgite Hydrogel Composite for Hg(II) Ions from Aqueous Solution

Xiaohuan Wang[1,2] and Aiqin Wang[1]
[1]*Center of Eco-Material and Green Chemistry, Lanzhou Institute of Chemical Physics, Chinese Academy of Sciences, Lanzhou, P. R. China*
[2]*Graduate University of the Chinese Academy of Sciences, Beijing, P. R. China*

Batch adsorption experiments were carried out to remove Hg(II) from aqueous solutions using chitosan-*g*-poly(acrylic acid)/ attapulgite hydrogel composites as adsorbents. The factors influencing the adsorption capacity of the composites were investigated. The results indicate that the adsorption equilibrium of the composites can be achieved within about ten minutes and the equilibrium adsorption capacities of the composites with 10, 30, and 50 wt% of attapulgite content were 785.20, 679.63, and 541.06 mg g^{-1}, respectively. The negative values of ΔG and positive values of ΔH indicate that the adsorption processes are all spontaneous and endothermic.

Keywords attapulgite; chitosan; Hg(II); hydrogel composite; thermodynamic parameter

INTRODUCTION

Mercury is a carcinogenic heavy metal. It can be accumulated in the body and may pose a potential threat to human health even at very low concentrations. It has been well documented that mercury may cause brain damage, dysfunction of liver, kidney, gastrointestinal tract and central nervous system, as well as induce cellular toxicity by binding to intracellular sulfhydryl groups (1–4). As a highly toxic element, the removal of mercury from wastewater has been receiving attention, especially in recent years (5–11). The processes commonly used for removing metal ions from industrial effluents include chemical precipitation (12), ion exchange (8,13), solvent extraction (11,14), reverse osmosis (15), adsorption (6,16,17), etc. Among various treatment methods, adsorption was found to be very effective, economical, versatile, and simple (18).

Received 7 April 2009; accepted 5 April 2010.
Address correspondence to Aiqin Wang, Center for Eco-Material and Green Chemistry, Lanzhou Institute of Chemical Physics, Chinese Academy of Sciences, Lanzhou 730000, China. Tel.: +86 931 4968118; Fax: +86 931 8277088. E-mail: aqwang@lzb.ac.cn

Activated carbon, as the most widely used adsorbent, also requires complexing agents to improve its removal performance for inorganic matters (19). The main disadvantages of using activated carbon as adsorbent are the high costs. In recent years, the research interest has been switching into the production of alternative adsorbents which have metal-binding capacities and are able to remove unwanted heavy metals from contaminated water at low cost. Natural materials, such as chitosan (20), zeolite (21), clay (10,22), or certain waste products from industrial operations such as fly ash (23), coal (24), and oxides (25), received much attention due to their low costs and local availability.

Chitosan (CTS), as a natural aminopolysaccharide, has received considerable interest for heavy metals removal due to its excellent metal-binding capacities and low cost as compared to activated carbon (19). However, CTS is a nonporous polymer. Its solubility in acid aqueous solutions also restricts its practical industrial application. So, modifications are needed to improve its adsorption performance and stability in acid aqueous solutions (20).

Attapulgite (APT), a crystalline hydrated magnesium silicate with a fibrous morphology, has a large specific surface area and moderate cation exchange capacity which is beneficial for the adsorption of heavy metals from solution. However, the adsorption capability of natural APT is very poor (26,27), some special treatments or modification, such as heat treatment, acid treatment (28), or graft reaction (29) are needed to enhance its adsorption performance and selectivity.

Recently, it is well documented that hydrogels with three-dimensional cross-linked polymeric networks could be used for the removal of metal ions from aqueous solutions (30–33), as hydrogels possess ionic functional groups such as carboxyls, amines, hydroxyls, and sulphonyl groups, which can adsorb and trap metal ions or ionic dyes from wastewater (30,31). However, most of the hydrogels are expensive synthetic polymers and their production

consumes lots of petroleum resources. Therefore, the design and synthesis of multi-component hydrogels based on natural materials have recently drawn considerable attention because such materials may not only exhibit improved performance but also show low costs and environmental friendly characteristics (34). So, in our current work, a series of chitosan-*g*-poly(acrylic acid)/attapulgite (CTS-*g*-PAA/APT) hydrogel composites were synthesized and used as adsorbents for the removal of Hg(II) from aqueous solutions. The factors influencing the adsorption capacity of the hydrogel composites for Hg(II) ions such as APT content (wt%), the initial pH value (pH_0) of the Hg(II) solutions, contact time (t), the initial concentration of Hg(II) solutions (C_0), and temperature (T) were studied. The characteristic parameters for the Langmuir isotherm model, the pseudo-first order and the pseudo-second order kinetic models have been determined, and thermodynamic parameters associated with the adsorption of the composites for Hg(II) were also calculated.

EXPERIMENTAL

Materials

Acrylic acid (AA, distilled under reduced pressure before use), ammonium persulfate (APS, recrystallized from distilled water before use), and *N,N′*-methylenebisacrylamide (MBA, used as received) were supplied by Shanghai Reagent Corp. (Shanghai, China). Chitosan (CTS, degree of deacetylation is 0.85, the average molecular weight is 3×10^5) was supplied by Zhejiang Yuhuan Ocean Biology Co. (Zhejiang, China). Natural Attapulgite (APT, supplied by Jiangsu Autobang International Co., Ltd., Jiangsu, China) was milled and sieved through a 320-mesh screen, and the cation exchange capacity (CEC) of the sample is 30.0 meq/100 g. Mercuric acetate (analytical grade reagent, $(CH_3COO)_2Hg$, 318.7) was supplied by Shanghai Reagent Corp. (Shanghai, China). Other reagents used were all of analytical grade reagents and all solutions were prepared with distilled water.

Preparation of CTS-*g*-PAA/APT Hydrogel Composites

CTS-*g*-PAA polymer and CTS-*g*-PAA/APT hydrogel composites were prepared according to our previous reports (35). The digital photo of CTS-*g*-PAA/APT composites was shown in Fig. 1. The products were milled and sieved through a 80-mesh screen.

Adsorption Experiments

In this study, all samples used for adsorption experiments have the same particle size. Each adsorption experiment was conducted in batch mode using 100 mL glass conical flasks equipped with glass stopples. 0.1000 g sample was mixed with 25 mL of mercuric acetate solution with the desired concentration and appropriate pH_0. The mixture was shaken in a thermostatic shaker bath (THZ-98A) with

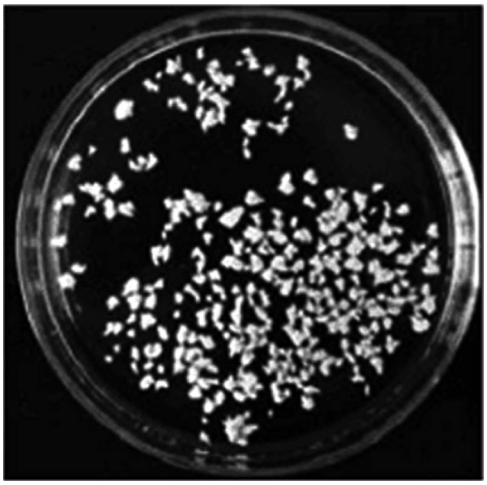

FIG. 1. The digital photo of CTS-*g*-PAA/APT composites.

120 rpm at the desired temperature for a given time. For the study of the effect of pH_0 of Hg(II) solution on adsorption, the pH_0 of Hg(II) solution was adjusted to different pH values (2.00, 3.00, 3.50, 4.00, 4.50, and 5.00) with acetic acid or sodium hydroxide solutions by using a Mettler Toledo 320 pH meter. Batch kinetic experiments were carried out at 303 K for predetermined time intervals (3, 5, 7, 9, 12, 15, 30, and 60 min) and the concentration of 3669 mg L^{-1} was selected as the initial concentration of Hg(II) solution. For temperature study, 0.1000 g sample was added into 25 mL Hg(II) solution (C_0 3625 mg L^{-1}, pH_0 5.00), and then the mixture was shaken at the temperature predetermined (293, 303, 313, 323, and 333 K) for 60 min to ensure the equilibrium to be established. For equilibrium adsorption experiments, 25 mL of various initial concentration of Hg(II) solution (pH_0 5.00) was mixed with 0.1000 g sample, and then the mixture was shaken at different temperature (293, 303, 313, 323, and 333 K) for 60 min to ensure the equilibrium to be established.

After adsorption, the Hg(II) solution was separated from the adsorbent by centrifugation at 5000 rpm for 10 min. The pH of each suspension was measured by a pH meter. Both the initial and the final concentrations of Hg(II) in the solutions were determined by EDTA titrimetric method using 0.0035 mol L^{-1} EDTA solution as the standard solution and 0.5% xylenol orange solution as the indicator. The amount of Hg(II) adsorbed at time t or at equilibrium by the material can be calculated by using Eq. (1).

$$q = [V(C_0 - C)]/m \tag{1}$$

where q is the amount of Hg(II) adsorbed at time t or at equilibrium (mg g^{-1}). C_0 is the initial concentration of Hg(II) solution (mg L^{-1}). C is the liquid-phase Hg(II)

concentration at time t or at equilibrium (mg L^{-1}). m is the mass of adsorbent used (g), and V is the volume of Hg(II) solution used (L).

Characterization

The BET specific surface area, the total pore volume, and the average pore size of the samples were measured using an Accelerated Surface Area and Porosimetry System (Micromeritics, ASAP 2020) by BET-method at 76 K. FTIR spectra measurements were done on a Thermo Nicolet NEXUS TM spectrophotometer using the KBr pellets. The spectrum was collected 32 times and corrected for the background noise.

RESULTS AND DISCUSSION

Effect of APT Content (wt%) on Adsorption Capacity

Under the same experimental conditions (C_0: 3800 mg L^{-1}; pH_0: 5.00; sample dose: 0.1000 g/25 mL; temperature: 303 K; contact time: 60 min), the equilibrium adsorption capacities (q_e) of CTS, natural APT, CTS-*g*-PAA and the composites for Hg(II) were determined, and the results were listed in Table 1. The experimental q_e values ($q_{e,exp}$) and the values calculated by the equilibrium adsorption capacities of APT and CTS-*g*-PAA of the composites ($q'_{e,cal}$) were also shown in Table 1. It can be seen from Table 1 that CTS is an excellent adsorbent for Hg(II). However, its solubility in acid aqueous solutions restricts its practical industrial application. The equilibrium adsorption capacity of natural APT and CTS-*g*-PAA were 13.20 mg g^{-1} and 837.99 mg g^{-1}, respectively. If APT and CTS-*g*-PAA were only compounded physically or mechanically, the equilibrium adsorption capacity of CTS-*g*-PAA/10%APT, CTS-*g*-PAA/30%APT and CTS-*g*-PAA/50%APT composite for Hg(II) should be 755.51, 590.55, and 425.60 mg g^{-1}, respectively. Obviously, there were differences between $q_{e,exp}$ and $q'_{e,cal}$, and the differences increased with the increase of wt%. This result indicates that the introduction of APT into CTS-*g*-PAA polymeric network can further improve the three-dimensional cross-linked polymeric networks and then enhance the adsorption capability of the composite for Hg(II) to some extent. In practical industrial production, one of the most important purposes of the addition of APT into polymers is to largely reduce the cost of adsorbents. Therefore, considering the economic advantage and the great adsorption capacity, CTS-*g*-PAA/APT composites may be very potential adsorbents for Hg(II).

TABLE 1
The comparison of the equilibrium adsorption capacities of the samples for Hg(II) under the same conditions (C_0: 3800 mg L^{-1}; pH_0: 5.00; sample dose: 0.1000 g/25 mL; temperature: 303 K; contact time: 60 min)

Samples	$q_{e,exp}$ (mg g^{-1})	$q'_{e,cal}$ (mg g^{-1})
CTS	712.62	–
APT	13.20	–
CTS-*g*-PAA	837.99	–
CTS-*g*-PAA/10%APT	785.20	755.51
CTS-*g*-PAA/30%APT	679.63	590.55
CTS-*g*-PAA/50%APT	541.06	541.06

Effect of pH_0 on Adsorption Capacity

Figure 2 showed the effect of pH_0 of mercuric acetate solution on the adsorption capacity of CTS-*g*-PAA and the composites for Hg(II). It can be seen from Fig. 2 that the adsorption capacities of CTS-*g*-PAA and the composites all increased when the pH_0 of solution increased from 2.00 to 5.00. However, the slope of each line was very small. In other words, the adsorption capacities of CTS-*g*-PAA and the composites all increased not very sharply with the increase of pH_0 of solution, which indicate that the adsorption of CTS-*g*-PAA and the composites for Hg(II) are not pH dependent. Such a phenomena can be substantiated by IR spectra of the representative CTS-*g*-PAA/30%APT composite after Hg(II) adsorption at pH_0 2.00 and 5.00. The spectra from Fig. 3 showed only little difference between the spectra at pH_0 2.00 and that at pH_0 5.00.

In order to explain the adsorption mechanism of CTS-*g*-PAA and the composites for Hg(II), IR spectra of the representative CTS-*g*-PAA and CTS-*g*-PAA/30%APT composite before and after Hg(II) adsorption were obtained. It can be seen from Fig. 4 that IR spectra of

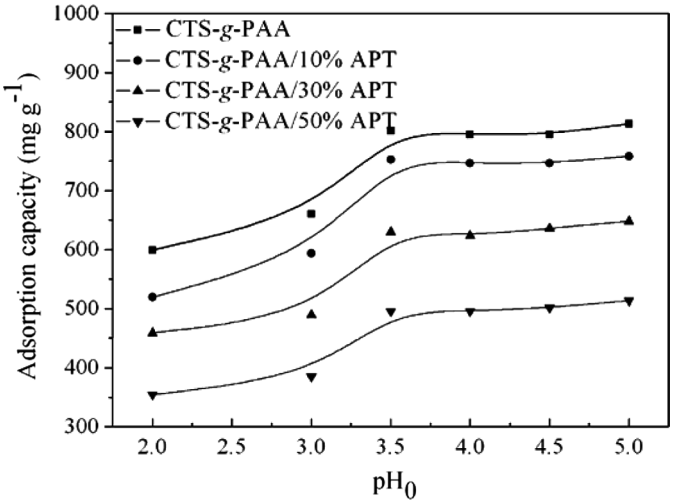

FIG. 2. Effect of pH_0 on the adsorption capacity of CTS-*g*-PAA and the composites for Hg(II). Adsorption experiments—C_0: 3693 mg L^{-1}; sample dose: 0.1000 g/25 mL; pH_0 range: 2.00 ~ 5.00; temperature: 303 K; adsorption time: 60 min.

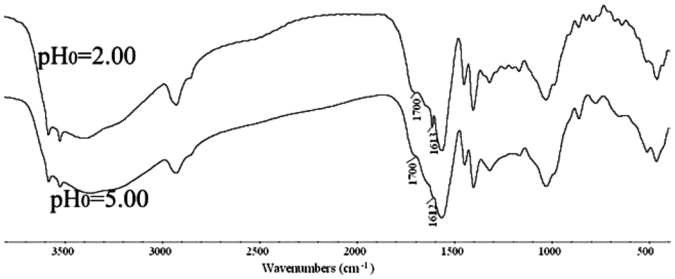

FIG. 3. IR spectra of the representative CTS-*g*-PAA/30%APT composite after Hg(II) adsorption at pH_0 2.00 and 5.00.

the sample after Hg(II) adsorption showed many variations. The major differences were listed as follows:

(i) the wide absorption band at near 3446 cm^{-1}, corresponding to the stretching vibration of $-NH_2$ groups and $-OH$ groups, widened and shifted to the lower wave numbers;
(ii) the strong absorption band at 1715 cm^{-1}, assigned to the stretching vibration of C=O of $-COOH$ groups, disappeared almost completely;
(iii) the absorption band at 1558 cm^{-1}, assigned to the stretching vibration of C=O of $-COO^-$ groups, was enhanced obviously and shifted to the higher wave numbers (1563 cm^{-1});
(iv) the absorption band at 1250 cm^{-1}, assigned to the deformation vibration absorption bands of $-OH$ groups, were enhanced obviously and shifted to the higher wave numbers (1320 cm^{-1}).

All of these changes in IR spectra of the representative CTS-*g*-PAA and CTS-*g*-PAA/30%APT composites before and after Hg(II) adsorption indicate that the adsorption of Hg(II) on the composites is a chemisorption, and $-COOH$, $-NH_2$, and –OH groups in the composites are all involved in the adsorption processes.

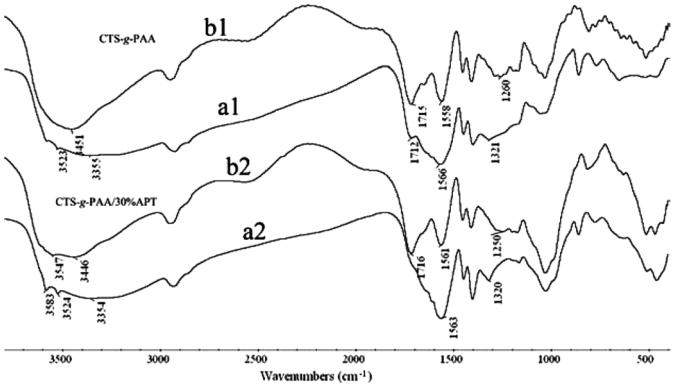

FIG. 4. IR spectra of the representative CTS-*g*-PAA (**1**) and CTS-*g*-PAA/30%APT composite (**2**) before (**b**) and after (**a**) Hg(II) adsorption.

Kinetic Studies

An ideal adsorbent for wastewater pollution control must not only have a large adsorption capacity but also a fast rate. In general, the adsorption capacity increases with contact time and, at some point in time, reaches a constant value. At this point, the amount of metal ions being adsorbed on the material is in a state of dynamic equilibrium with the amount of metal ions desorbed from the adsorbent. Figure 5 showed the effect of contact time on the adsorption capacity of CTS-*g*-PAA and the composites for Hg(II). Obviously, the Hg(II) adsorption rates on the composites were very fast. The adsorption equilibrium of the composites can be reached within about 10 minutes. The sequence of adsorption rate is: CTS-*g*-PAA/30%APT >CTS-*g*-PAA/10%APT ≈ CTS-*g*-PAA/50%APT > CTS-*g*-PAA. Such results are just consistent with the results of the BET specific surface area, the total pore volume, and average pore size of CTS-*g*-PAA and the composites (shown in Table 2). Such a phenomenon suggests that the BET specific surface area, total pore volume, and average pore size of the samples are important factors influencing the adsorption rate. In order to make sure all samples reach adsorption equilibrium completely, 60 min was selected as the contact time for the adsorption of Hg(II) on CTS-*g*-PAA and the composites under our experimental conditions.

Several kinetic models can be used to describe the adsorption kinetics. In this study, three common equations were tested to find the best-fitted model for the experimental data obtained, namely, the pseudo-first order and the pseudo-second order kinetic models and the intraparticle diffusion model. The corresponding linear equations are given below.

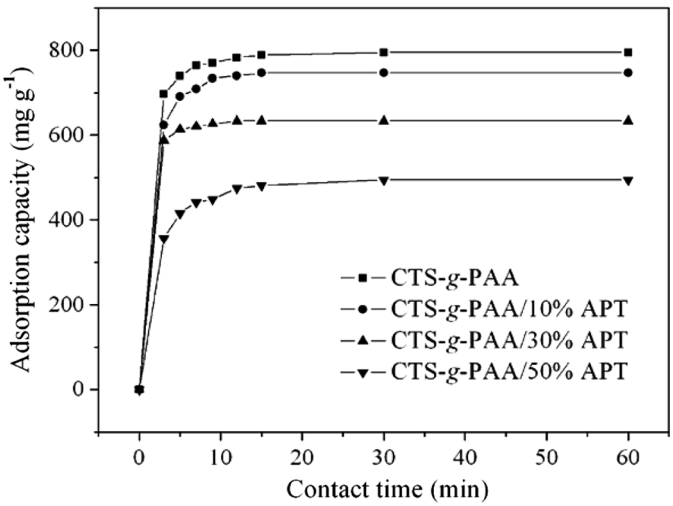

FIG. 5. Effect of contact time on the adsorption capacity of CTS-*g*-PAA and the composites for Hg(II). Adsorption experiments—C_0: 3669 mg L^{-1}; sample dose: 0.1000 g/25 mL; pH_0: 5.00; temperature: 303 K.

TABLE 2
The BET specific surface area, total pore volume and average pore width for CTS-*g*-PAA and the composites

Sample	BET specific surface area ($m^2 g^{-1}$)	Total pore volume ($cm^3 g^{-1}$)	Adsorption average pore width (nm)
CTS-*g*-PAA	1.83	0.0041	8.99
CTS-*g*-PAA/10%APT	8.38	0.0343	16.35
CTS-*g*-PAA/30%APT	24.66	0.0995	16.13
CTS-*g*-PAA/50%APT	9.85	0.0284	11.54

The pseudo-first order kinetic model was suggested by Lagergren (36) for the adsorption of solid/liquid systems and its linear form can be formulated as:

$$\log(q_e - q_t) = \log(q_e) - k_1 t/2.303 \quad (2)$$

Ho and McKay's pseudo-second order kinetic model (37) can be expressed as:

$$t/q_t = 1/(k_2 q_e^2) + t/q_e \quad (3)$$

where q_e and q_t are the amount of Hg(II) adsorbed at equilibrium and time t ($mg\,g^{-1}$), respectively. k_1 is the equilibrium rate constant of the pseudo-first order adsorption (min^{-1}). k_2 is the equilibrium rate constant of the pseudo-second order adsorption ($g\,mg^{-1}\,min^{-1}$). By testing the plots of $\log(q_e - q_t)$ versus t and t/q_t versus t (plots not shown), the rate constants k_1, k_2 and correlation coefficients can be calculated and the results were listed in Table 3.

As can be seen from Table 3, the linear correlation coefficients (R^2) of the pseudo-first order kinetic model of CTS-*g*-PAA/10%APT composite and CTS-*g*-PAA/50%APT composite are very high, and there are large differences between their experimental q_e values ($q_{e,exp}$) and their calculated q_e values ($q_{e,cal}$). Meanwhile, R^2 of the pseudo-first order kinetic model of CTS-*g*-PAA and CTS-*g*-PAA/50%APT composite are low, and the differences between their $q_{e,exp}$ values and their $q_{e,cal}$ values are very obvious. All of these indicate that the pseudo-first order kinetic model was poor fit for the adsorption processes of CTS-*g*-PAA and the composites for Hg(II). It can also be seen from Table 3 that R^2 of the pseudo-second order kinetic model of CTS-*g*-PAA and the composites are all over 0.9998. Moreover, their $q_{e,cal}$ values of the pseudo-second order kinetic model are all consistent with their $q_{e,exp}$ values. These results suggest that the adsorption processes of CTS-*g*-PAA and the composites for Hg(II) can be well described by the pseudo-second order kinetic model.

The intraparticle diffusion kinetics model can be formulated as (38):

$$q_t = k_i t^{1/2} + C \quad (4)$$

where k_i ($mg\,g^{-1}\,min^{-1/2}$) is the intraparticle diffusion rate constant and C ($mg\,g^{-1}$) is a constant. If the process is considered to be influenced by diffusion in the particles and convective diffusion in the solution, the mathematical dependence of q_t versus $t^{1/2}$ can be obtained (38). The plots of q_t versus $t^{1/2}$ were shown in Fig. 6. As seen from Fig. 6, the plots were not linear over the whole time range, which lead us to conclude that the intraparticle diffusion kinetic model was poor fit for the adsorption processes of CTS-*g*-PAA and the composites for Hg(II).

Adsorption Isotherms

Figure 7 showed the influence of C_0 on the adsorption capacities of CTS-*g*-PAA and the composites for Hg(II)

TABLE 3
Constants and correlation coefficients of the pseudo-first order and pseudo-second order models for Hg(II) adsorption on CTS-*g*-PAA and the composites

	Pseudo-first order model				Pseudo-second order model		
Samples	$q_{e,exp}$ ($mg\,g^{-1}$)	$q_{e,cal}$ ($mg\,g^{-1}$)	k_1 (min^{-1})	R^2	$q_{e,cal}$ ($mg\,g^{-1}$)	k_2 ($g\,mg^{-1}\,min^{-1}$)	R^2
CTS-*g*-PAA	795.01	687.54	0.3445	0.8838	833.33	0.0036	1
CTS-*g*-PAA/10%APT	746.09	516.89	0.3929	0.9718	769.23	0.0042	0.9999
CTS-*g*-PAA/30%APT	633.59	356.20	0.4852	0.9166	625.00	0.0128	1
CTS-*g*-PAA/50%APT	495.03	327.47	0.2287	0.9559	500.00	0.0021	0.9998

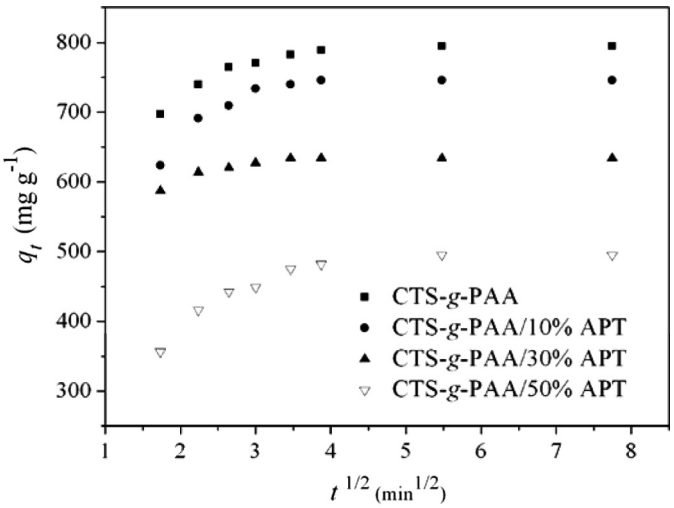

FIG. 6. The intraparticle diffusion rate model for Hg(II) adsorption on CTS-*g*-PAA and the composites.

at 303 K. It is clear that C_0 plays an important role in the adsorption processes. The adsorption capacities increased rapidly with the increase of C_0, which may be due to the fact that the increase in Hg(II) concentration leads to the increase in the driving force of the concentration gradient, and then accelerates the diffusion of Hg(II) ions on the adsorbent.

Adsorption isotherms describe how adsorbate molecules interact with adsorbent particles, so, are critical in optimizing the use of adsorbents. It is possible to depict the equilibrium adsorption isotherms by plotting the Hg(II) concentration in the solid phase versus that in the liquid phase. The distribution of Hg(II) ions between the liquid phase and the adsorbent is a measurement of the position of equilibrium in the adsorption process. An accurate mathematical description of equilibrium adsorption capacity is indispensable for reliable prediction of adsorption parameters and quantitative comparison of adsorption behaviour for different adsorbent systems (or for varied experimental conditions) within any given system (39). In the present study, the adsorption data is interpreted by using the well-known and widely applied isotherm equation, namely, the Langmuir isotherm model. The Langmuir model is based on the assumption of a structurally homogeneous adsorbent where all sorption sites are identical and energetically equivalent.

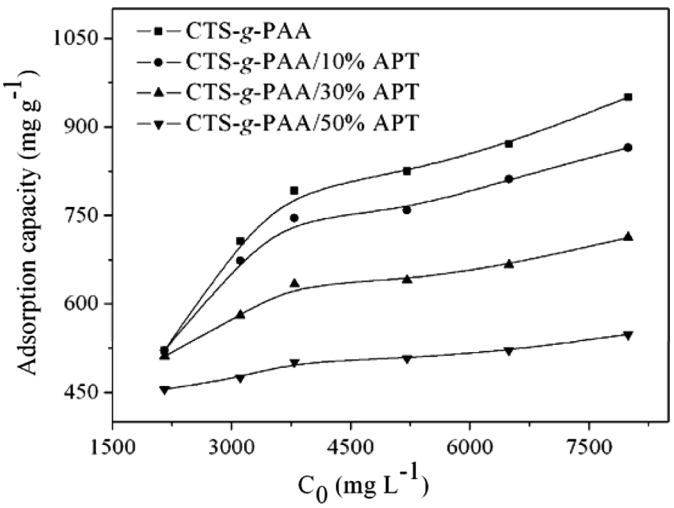

FIG. 7. Effect of the initial concentration (C_0) of Hg(II) on the adsorption capacity of CTS-*g*-PAA and the composites for Hg(II). Adsorption experiments—sample dose: 0.1000 g/25 mL; pH_0: 5.00; temperature: 303 K; contact time: 60 min.

The Langmuir equation is represented as follows (40):

$$q_e = x/m = K_L C_e/(1 + a_L C_e) \tag{5}$$

And its linear form is formulated as:

$$C_e/q_e = 1/K_L + (a_L/K_L)C_e \tag{6}$$

where x is the amount of Hg(II) adsorbed (mg); m is the amount of adsorbent used (g); C_e (mg L^{-1}) and q_e (mg g^{-1}) are the liquid phase concentration and solid phase concentration of adsorbate at equilibrium; K_L (L g^{-1}) and a_L (L mg^{-1}) are the Langmuir isotherm constants. Langmuir isotherm constants, K_L and a_L, can be evaluated through the linear form of the Langmuir equation (shown in Eq. (6)). By plotting C_e/q_e against C_e, it is possible to obtain the value of K_L from the intercept which is $1/K_L$ and the value of a_L from the slope which is a_L/K_L. The maximum adsorption capacity of the adsorbent, $q_{m,cal}$, (equilibrium monolayer capacity or saturation capacity) is numerically equal to K_L/a_L.

The Langmuir parameters of CTS-*g*-PAA and the composites for Hg(II) at different temperatures obtained from the plots of C_e/q_e versus C_e (plots not shown) were listed in Table 4. It is obvious that the linearized forms of the isotherms are found to be linear over the whole concentration range studied and the correlation coefficients (R^2) were extremely high, which strongly support the fact that the adsorption data of Hg(II) on CTS-*g*-PAA and the composites closely follow the Langmuir model of adsorption.

It can also be seen from Table 4 that temperature has a positive influence on the Hg(II) amount adsorbed. Moreover, at all the tested temperatures, the values of ΔG are all negative and decrease with the increase of temperature. All of these indicate the endothermic and spontaneous nature of the adsorption of CTS-*g*-PAA and the composites for Hg(II) and the spontaneous nature may be enhanced at higher temperature.

TABLE 4
Langmuir isotherm constants, correlation coefficients and Gibbs free energy changes associated with the adsorption of Hg(II) on CTS-*g*-PAA and the composites at different temperatures (T: K; K_L: L g^{-1}; $q_{m,cal}$: mg g^{-1}; ΔG: kJ mol^{-1})

	CTS-*g*-PAA				CTS-*g*-PAA/10%APT				CTS-*g*-PAA/30%APT				CTS-*g*-PAA/50%APT			
T	K_L	$q_{m,cal}$	ΔG	R^2	K_L	$q_{m,cal}$	ΔG	R^2	K_L	$q_{m,cal}$	ΔG	R^2	K_L	$q_{m,cal}$	ΔG	R^2
293	75.643	892.86	−10.54	0.9997	46.232	826.44	−9.34	0.9996	26.192	740.74	−7.96	0.9996	11.069	588.23	−5.86	0.9993
303	74.349	900.90	−10.85	0.9997	45.767	840.34	−9.63	0.9997	27.724	746.27	−8.37	0.9996	11.937	591.72	−6.25	0.9994
313	90.909	909.09	−11.74	0.9998	49.751	854.70	−10.17	0.9998	29.395	751.87	−8.8	0.9996	11.206	598.79	−6.29	0.9993
323	108.225	917.43	−12.58	0.9998	57.143	862.07	−10.86	0.9998	34.941	751.88	−9.54	0.9997	12.467	602.40	−6.78	0.9994
333	116.686	917.43	−13.18	0.9998	66.225	862.07	−11.61	0.9998	37.397	757.58	−10.03	0.9997	15.333	602.42	−7.56	0.9995

Thermodynamic Parameters

Generally speaking, the adsorption of pollutants increases with temperature because high temperatures provide a faster rate of diffusion of adsorbate molecules from the solution to the adsorbent (41). With the increase of temperature, the solubility of the solute increases. Meanwhile, the increase in temperature may cause the increase of the chemical potential of the material. The investigation of the influence of temperature on adsorption can also help to confirm the thermodynamic parameters. Table 5 showed the results about the equilibrium adsorption capacities of CTS-*g*-PAA and the composites for Hg(II) changed with the temperature under the same experimental conditions (C_0: 3624.69 mg L^{-1}; pH$_0$: 5.00; sample dose: 0.1000 g/25 mL; contact time: 60 min). It can be seen that the equilibrium adsorption capacities of CTS-*g*-PAA and the composites for Hg(II) all increased with the increase of temperature. Such results also indicate that high temperature is in favor of the adsorption of CTS-*g*-PAA and the composites for Hg(II). In other words, the adsorption processes of CTS-*g*-PAA and the composites for Hg(II) are all endothermic processes.

In order to further substantiate our prediction about the endothermic nature of the adsorption processes of CTS-*g*-PAA and the composites for Hg(II), thermodynamic parameters such as Gibbs free energy change (ΔG, J mol^{-1}) (shown in Table 4), enthalpy change (ΔH, J mol^{-1}), and entropy change (ΔS, J mol^{-1} K^{-1}) were calculated. And such thermodynamic parameters were calculated by Gibbs equation and Van't Hoff equation (listed as follows) (42,43).

$$\Delta G = -RT \ln K_L \tag{7}$$

$$\ln K_L = -\Delta H/RT + \Delta S/R \tag{8}$$

where K_L is Langmuir isotherm constant (L g^{-1}) and the value of K_L can be evaluated through the linear form of the Langmuir equation (shown in Eq. (6)). T (K) is the temperature, R (J mol^{-1} K^{-1}) is the gas constant. The values of ΔH and ΔS were determined from the slopes and intercepts of the plots of $\ln K_L$ versus $1/T$ (Plots not shown).

Thermodynamic parameters associated with the adsorption of CTS-*g*-PAA and the composites for Hg(II) were listed in Table 6. The positive values of ΔH confirmed that the adsorption of CTS-*g*-PAA and the composites for Hg(II) are all endothermic processes, which are consistent with the results of the influence of temperature on adsorption. The positive value of ΔS showed that the randomness at the solid-liquid interface increased during the adsorption processes of Hg(II) on CTS-*g*-PAA and the composites.

TABLE 5
The relationship between temperature and the equilibrium adsorption capacity of CTS-*g*-PAA and the composites for Hg(II)

	$q_{e,exp}$ (mg g^{-1})				
Samples	293 K	303 K	313 K	323 K	333 K
CTS-*g*-PAA	818.20	822.59	826.99	831.39	840.19
CTS-*g*-PAA/10%APT	765.41	769.81	774.21	783.00	787.40
CTS-*g*-PAA/30%APT	637.84	651.04	655.44	664.23	668.63
CTS-*g*-PAA/50%APT	514.67	519.07	527.87	532.27	536.67

TABLE 6
Thermodynamic parameters associated with the adsorption of CTS-*g*-PAA and the composites for Hg(II)

Samples	Equations	R^2	ΔH ($kJ\,mol^{-1}$)	ΔS ($kJ\,mol^{-1}\,K^{-1}$)
CTS-*g*-PAA	$\ln K_L = 8.3781–1205.8512\ (1/T)$	0.9575	10.025	0.070
CTS-*g*-PAA/10%APT	$\ln K_L = 6.8595–905.5046\ (1/T)$	0.9328	7.528	0.057
CTS-*g*-PAA/30%APT	$\ln K_L = 6.3599–915.5835\ (1/T)$	0.9727	7.612	0.053
CTS-*g*-PAA/50%APT	$\ln K_L = 4.6377–664.4018\ (1/T)$	0.8173	5.524	0.037

CONCLUSIONS

The following conclusions can be obtained on the basis of the experimental results obtained from the adsorption of Hg(II) on the composites:

(1) The adsorption of Hg(II) on the composites is a chemisorption, and $-COOH$, $-NH_2$, and –OH groups in the composites were all involved in the adsorption processes. Even at the very low pH_0 value (pH_0 2.00), the composites can also adsorb large amount of Hg(II).
(2) The Hg(II) adsorption rate of the composites was fast and the equilibrium adsorption capacities of the composites with 10, 30, and 50 wt% of APT content were 785.20, 679.63, and 541.06 $mg\,g^{-1}$, respectively. The adsorption processes of the composites for Hg(II) were all better fitted for the pseudo-second order model and the Langmuir model, respectively.
(3) The values of ΔG of the adsorption of the composites for Hg(II) are all negative, which indicates the spontaneous nature of the adsorption processes. The positive values of ΔH confirmed that the adsorption of the composites for Hg(II) are all endothermic processes. The positive value of ΔS showed that the randomness at the solid-liquid interface increased during the adsorption processes of Hg(II) on the composites.
(4) The introduction of APT into CTS-*g*-PAA polymeric networks not only improved the adsorption ability and adsorption rate of the composites, but also reduced the cost of adsorbents. Meanwhile, the preparation of the composites also improved the stability of CTS in acid aqueous solutions.

The results above showed that the composites may be used as a novel type, not pH dependent, fast-responsive, and high-capacity sorbent material for Hg(II).

ACKNOWLEDGEMENTS

The authors thank for joint support by the National Natural Science Foundation of China (No.20877077), Taihu Project of Jiangsu Provincial Sci. & Tech. Department (No. BS2007118) and Science and Technology Support Project of Gansu Provincial Sci. & Tech. Department (No. 0804GKCA03A).

REFERENCES

1. Namasivayam, C., Kadirvelu, K. (1999) Uptake of mercury(II) from wastewater by activated carbon from an unwanted agricultural solid by-product: Coirpith. *Carbon*, 37: 79–84.
2. USEPA (2001) National Primary Drinking Water Standards. Report EPA 816-F-01-007, United States Environmental Protection Agency, Washington, DC.
3. Yavuz, H., Denizli, A., Güngüneş, H., Safarikova, M., Safarik, I. (2006) Biosorption of mercury on magnetically modified yeast cells. *Sep. Purif. Technol.*, 52: 253–260.
4. Zhang, F.S., Nriagu, J.O., Itoh, H. (2005) Mercury removal from water using activated carbons derived from organic sewage sludge. *Water Res.*, 39: 389–395.
5. Bilba, D., Bilba, N., Moroi, G. (2007) Removal of mercury(II) ions from aqueous solutions by the polyacrylamidoxime chelating fiber. *Sep. Sci. Technol.*, 42: 171–184.
6. Rao, M.M., Reddy, D.H.K.K., Venkateswarlu, P., Seshaiah, K. (2009) Removal of mercury from aqueous solutions using activated carbon prepared from agricultural by-product/waste. *J. Environ. Manage.*, 90: 634–643.
7. Karabulut, S., Karabakan, A., Denizli, A., Yürüm, Y. (2001) Cadmium(II) and mercury(II) removal from aquatic solutions with low-rank turkish coal. *Sep. Sci. Technol.*, 36 (16): 3657–3671.
8. Anirudhan, T.S., Divya, L., Ramachandran, M. (2008) Mercury(II) removal from aqueous solutions and wastewaters using a novel cation exchanger derived from coconut coir pith and its recovery. *J. Hazard. Mater.*, 157: 620–627.
9. Anirudhan, T.S., Radhakrishnan, P.G., Suchithra, P.S. (2008) Adsorptive removal of mercury(II) ions from water and wastewater by polymerized tamarind fruit shell. *Sep. Sci. Technol.*, 43: 3522–3544.
10. Dias Filho, N.L., do Carmo, D.R. (2006) Study of an organically modified clay: Selective adsorption of heavy metal ions and voltammetric determination of mercury(II). *Talanta*, 68: 919–927.
11. Khalid, N., Ahmad, S., Kiani, S.N., Ahmed, J. (1999) Removal of mercury from aqueous solutions by adsorption to rice husks. *Sep. Sci. Technol.*, 34 (16): 3139–3153.
12. Charerntanyarak, L. (1999) Heavy metals removal by chemical coagulation and precipitation. *Water Sci. Technol.*, 39: 135–138.
13. Dąbrowski, A., Hubicki, Z., Podkościelny, P., Robens, E. (2004) Selective removal of the heavy metal ions from waters and industrial wastewaters by ion-exchange method. *Chemosphere*, 56: 91–106.
14. Silva, J.E., Paiva, A.P., Soares, D., Labrincha, A., Castro, F. (2005) Solvent extraction applied to the recovery of heavy metals from galvanic sludge. *J. Hazard. Mater.*, 120: 113–118.
15. Benito, Y., Ruiz, M.L. (2002) Reverse osmosis applied to metal finishing wastewater. *Desalination*, 142: 229–234.
16. Demirbas, A. (2008) Heavy metal adsorption onto agro-based waste materials: A review. *J. Hazard. Mater.*, 157: 220–229.
17. Namasivayam, C., Senthilkumar, S. (1997) Recycling of industrial solid waste for the removal of mercury (II) by adsorption process. *Chemosphere*, 34: 357–375.

18. Mohanty, K., Das, D., Biswas, M.N. (2006) Preparation and characterization of activated carbons from *Sterculia alata* nutshell by chemical activation with zinc chloride to remove phenol from wastewater. *Adsorption*, 12: 119–132.
19. Sandhya, B., Tonni, A.K. (2003) Low-cost adsorbents for heavy metals uptake from contaminated water: A review. *J. Hazard. Mater.*, 97: 219–243.
20. Crini, G., Badot, P.-M. (2008) Application of chitosan, a natural aminopolysaccharide, for dye removal from aqueous solutions by adsorption processes using batch studies: A review. *Prog. Polym. Sci.*, 33: 399–447.
21. Erdem, E., Karapinar, N., Donat, R. (2004) The removal of heavy metal cations by natural zeolites. *J. Colloid Interface Sci.*, 280: 309–314.
22. Potgieter, J.H., Potgieter-Vermaak, S.S., Kalibantonga, P.D. (2006) Heavy metals removal from solution by palygorskite clay. *Miner. Eng.*, 19: 463–470.
23. Rio, S., Delebarre, A. (2003) Removal of mercury in aqueous solution by fluidized bed plant fly ash. *Fuel*, 82: 153–159.
24. Hoffart, A., Seames, W., Kozliak, E., Riedinger, S., Francini, J., Carlson, C. (2006) A two-step acid mercury removal process for pulverized coal. *Fuel*, 85: 1166–1173.
25. Wu, S., Uddin, M.A., Sasaoka, E. (2006) Characteristics of the removal of mercury vapor in coal derived fuel gas over iron oxide sorbents. *Fuel*, 85: 213–218.
26. Chen, H., Wang, A. (2007) Kinetic and isothermal studies of lead ion adsorption onto palygorskite clay. *J. Colloid Interface Sci.*, 307: 309–316.
27. Wang, W., Chen, H., Wang, A. (2007) Adsorption characteristics of Cd(II) from aqueous solution onto activated palygorskite. *Sep. Purif. Technol.*, 55: 157–164.
28. Chen, H., Zhao, Y., Wang, A. (2007) Removal of Cu(II) from aqueous solution by adsorption onto acid-activated palygorskite. *J. Hazard. Mater.*, 149: 346–354.
29. Liu, P., Wang, T. (2007) Adsorption properties of hyperbranched aliphatic polyester grafted attapulgite towards heavy metal ions. *J. Hazard. Mater.*, 149: 75–79.
30. Yetimoğlu, E.K., Kahraman, M.V., Ercan, Ö, Akdemir, Z.S., Apohan, N.K. (2007) *N*-vinylpyrrolidone/acrylic acid/2-acrylamido-2-methylpropane sulfonic acid based hydrogels: Synthesis, characterization and their application in the removal of heavy metals. *React. Funct. Polym.*, 67: 451–460.
31. Bekiari, V., Sotiropoulou, M., Bokias, G., Lianos, P. (2008) Use of poly(*N,N*-dimethylacrylamide-co-sodium acrylate) hydrogel to extract cationic dyes and metals from water. *Colloids Surf. A: Physicochem. Eng. Aspects*, 312: 214–218.
32. Kagöz, H., Özgümü, S., Orbay, M. (2001) Preparation of modified polyacrylamide hydrogels and application in removal of Cu(II) ion. *Polymer*, 42: 7497–7502.
33. Kagöz, H., Özgümü, S., Orbay, M. (2003) Modified polyacrylamide hydrogels and their application in removal of heavy metal ions. *Polymer*, 44: 1785–1793.
34. Chen, H., Wang, A. (2008) Adsorption characteristics of Cu(II) from aqueous solution onto poly(acrylamide)/attapulgite composite. *J. Hazard. Mater.*, 165: 223–231.
35. Zhang, J., Wang, Q., Wang, A. (2007) Synthesis and characterization of chitosan-*g*-poly(acrylic acid)/attapulgite superabsorbent composites. *Carbohydr. Polym.*, 68: 367–374.
36. Lagergren, S. (1898) About the theory of so-called adsorption of soluble substances. Kungliga Svenska Vetenskapsakademiens. *Handlingar*, 24: 1–39.
37. Ho, Y.S., McKay, G. (1999) Pseudo-second order model for sorption processes. *Process Biochem.*, 34: 451–465.
38. Weber, W.J., Morris, J.J. (1963) Kinetics of adsorption on carbon from solution. *J. Sanitary Eng. Div. Proc. Am. Soc. Civil Eng. SA2*, 89: 31–59.
39. Ahluwalia, S.S., Goyal, D. (2007) Microbial and plant derived biomass for removal of heavy metals from wastewater. *Bioresour. Technol.*, 98: 2243–2257.
40. Langmuir, I. (1916) The constitution and fundamental properties of solids and liquids. *J. Am. Chem. Soc.*, 38: 2221–2295.
41. Bernardin, Jr., F.E. (1985) Experimental Design and Testing of Adsorption and Adsorbates. In: *Adsorption Technology: A Step-by-Step Approach to Process Evaluation and Application*, Slejko, F.L., ed.; Marcel Dekker, Inc., New York, Basel, 37–90.
42. Renault, F., Morin-Crini, N., Gimbert, F., Badot, P.M., Crini, G. (2008) Cationized starch-based material as a new ion-exchanger adsorbent for the removal of C.I. Acid Blue 25 from aqueous solutions. *Bioresour. Technol.*, 99: 7573–7586.
43. Ho, Y.S., Ofomaja, A.E. (2006) Biosorption thermodynamics of cadmium on coconut copra meal as biosorbent. *Biochem. Eng. J.*, 30: 117–123.